Trans. Phenom. Nano Micro Scales, 8(1): 9-22, Winter and Spring 2020
DOI: 10.22111/tpnms.2019.29314.1172

ORIGINAL RESEARCH PAPER

MHD Jeffrey NanoFluids Flow Over a Stretching Sheet Through a Porous Medium in Presence of Nonlinear Thermal Radiation and Heat Generation/Absorption

Ramadan Abdullah Mohamed [1], Abdelraheem Mahmoud Aly [1,2], Sameh Elsayed Ahmed [,1,2] , Mahmoud Sayed Soliman [1]*

[1]Department of mathematics, Faculty of science, South valley university, Qena, Egypt
[2]Department of Mathematics, Faculty of Science, Abha, King Khalid University, Saudi Arabia

Received 18 March 2019; revised 28 November 2019; accepted 10 December 2019; available online 22 February 2020

ABSTRACT: In this article, a numerical investigation of magnetohydrodynamic non-Newtonian nanofluid flow on a stretching sheet through an isotropic porous medium. The effects of both non-linear thermal radiation and heat generation/absorption were studied on distributions of velocity, temperature and concentration. On the other side, the governing partial differential equations have been transformed by using suitable similarity transformations into a system of ordinary differential equations and then solved, numerically by using the fourth order Runge-Kutta method with shooting technique. The principal findings of the study showed up that the effect of both Darcy number and magnetic field on the velocity profile is decreasing, while the impacts of both non-linear thermal radiation and heat source/skin on temperature are increasing and decreasing on concentration distribution respectively. Numerical solutions were calculated for the skin fraction, local Nusselt number and local Sherwood number for values of all important physical parameters.

KEYWORDS: *Magnetohydrodynamic (MHD); Nanofluid; Porous media; Stretching surface; Thermal radiation*

INTRODUCTION

The key building blocks of nanofluids are nanoparticles; so research on nanofluids got accelerated because of the development of nanotechnology in general and availability of nanoparticles in particular. Compared to micrometer sized particles, nanoparticles possess high surface area to volume ratio due to the occupancy of large number of atoms on the boundaries, which make them highly stable in suspensions. Thus the Nano-suspensions show high thermal conductivity possibly due to enhanced convection between the solid particle and liquid surfaces. Since the properties like the thermal conductivity of the Nano-sized materials are typically an order of magnitude higher than those of the base fluids, nanofluids show enhancement in their effective thermal properties. Due to the lower dimensions, the dispersed nanoparticles can behave like a base fluid molecule in a suspension, which helps us to reduce problems like particle clogging, sedimentation etc. Nanofluids have many applications and uses in fields of the medicine such as nanoparticles treatment against cancer as well as in various types of industries as well as in the field of pharmacy. It, also has important uses in the process of thermal transitions, for example, as refrigerants in thermal transfer equipment and cooling system in electronic devices. Gangaiah et al. [1] studied magneto hydrodynamic flow of nanofluid over an exponentially stretching sheet in presence of viscous dissipation and chemical reaction.

*Corresponding Author Email: *sehassan@kku.edu.sa*
Tel.: +966544186317; Note. This manuscript was submitted on March 18, 2019; approved on December 10, 2019; published online 22 February 2020, 2020.

Farooq et al. [2] examined melting heat transfer and double stratification in stagnation flow of viscous nanofluid.

Hsiao [3] flexed analyze stagenation electrical MHD nanofluid mixed convection with slip boundary on a stretching sheet. Mabood et al. [4] discussed framing the features of Brownian motion and thermophoresis on radiative nanofluid flow past a rotating stretching sheet with magnetohydrodynamic.

Ansari et al. [5] computed a new numerical approach to MHD Maxwellian nanofluid flow past an impulsively stretching sheet. Nampelly et al. [6] explained thermal radiation and slip effects on MHD flow and heat transfer of Casson nanofluid over an exponentially stretching sheet. Goyal and Bhargava [7] computed the boundary layer flow and heat transfer of viscoelastic nanofluids past a stretching sheet with partial slip conditions. Krishnamurthy et al. [8] resolved the effect of chemical reaction on MHD boundary layer flow and melting heat transfer of Williamson nanofluid in porous medium.

Bhargava and Rana [9] dissected the finite element analysis of viscoelastic nanofluid flow with energy dissipation and internal heat Source/Sink effects. Madhua and Kishanb [10] debated the finite element analysis of MHD viscoelastic nanofluid flow over a stretching sheet with radiation. Study of magnetohydrodynamic (MHD) flow of an electrically conducting fluid due to the stretching of the sheet is of considerable interest in modern metallurgical and metalworking processes.

Nomenclature

C	nanoparticles volume fraction	Sh	local Sherwood
C_f	skin fraction	T	temperature of fluid
Ct	ratio temperature	T_w	temperature of wall
C_w	nanoparticles fraction at wall	u, v	velocity components
Da	Darcy number	x,y	space coordinates
D_B	Brownian diffusion coefficient		**Greek Symbols**
D_T	thermophoresis diffusion coefficient	α	thermal diffusivity
k*	mean absorption coefficient	β	Deborah number
Le	Lewis number	η	similarity variable
M	magnetic field	θ	dimensionless temperature
Nb	Brownian motion	λ	ratio of relaxation to radiation times
Nt	Thermophoresis	λ_1	retardation time
Nu	Local Nusselt number	ν	kinematic viscosity
Pr	Prandtl number	ρ	density of the fluid
q_m	mass flux	$(\rho c)_f$	heat capacity of the base fluid
q_r	nonlinear radiative heat flux	ρ_{cp}	density of base fluid
q_w	heat flux	$(\rho c)_p$	heat capacity of a nanoparticle
R	Thermal radiation	σ^*	Stefan-Boltzmann constant
Re_x	local Reynolds number	τ	parameter defined by the ratio
S	heat source/sink	ϕ	dimensionless concentration function
		ψ	dimensionless stream function

Many metallic materials are manufactured after they have been refined sufficiently in the molten state. The study of the flow and heat transfer in an electrically conducting fluid permeated by a transverse magnetic field is of special interest and has many practical applications in manufacturing processes in industry. Study of MHD heat transfer field can be divided into two classes, in the first class the electromagnetic fields use to control the heat transfer as in the convection flows and aerodynamic heating, while in the second class the heating is produced by electromagnetic fields for example in generators, pumps, etc. Chanie et al. [11] reported MHD flow of nanofluids through a porous medium due to a permeable stretching sheet. Gaikwad and Chillal [12] expounded radiation effect on MHD mixed convective flow of Cu/CuO-water Nano fluids in the presence of chemical reaction. Thumma and Mishra [13] anatomized effect of viscous dissipation and joule heating on magneto hydrodynamic Jeffery Nano fluid flow with and without multi slip boundary conditions. zeid [14] analyzed the effects of thermal-diffusion and viscous dissipation on peristaltic flow of micro polar non-Newtonian nanofluid. Mliki et al. [15] illustrated instability of Lattice Boltzmann simulation of natural convection in an L-shaped enclosure in the presence of nanofluid. Mohamed et al. [16] investigated MHD flow of Sisko fluid over a bidirectional radiating stretching surface embedded in a nanofluid saturated porous media in the presence of heat generation/absorption and chemical reaction. Baag et al. [17] reported magnetohydrodynamic boundary layer flow over an exponentially stretching sheet past a porous medium with uniform heat source. Eldabe et al. [18] illuminated peristaltic flow of MHD Jeffrey fluid through porous medium in a vertical channel with heat and mass transfer with radiation. Kiran [19] explained nonlinear thermal convection in a viscoelastic Nano fluid saturated porous medium under gravity modulation. Naramgari and Sulochana [20] excogitated MHD flow of dusty nanofluid over a stretching surface with volume fraction of dust field on temperature is increasing. In fluid mechanics, fluid flow through porous media is the manner in which fluids behave when flowing through a porous medium, for example sponge or wood, or when filtering water using sand or another porous material. As commonly observed, some fluid flows through the media while some mass of the fluid is stored in the pores present in the media. Uddin et al. [21] accentuated the finite element simulation of magneto hydrodynamic convective nanofluid slip flow in a porous medium with nonlinear thermal radiation. Ganesh et al. [22] discussed the Lie symmetry group analysis of magnetic field effects on free convective flow of a nanofluid over a semi-infinite stretching sheet. Huda et al [23] elucidated dynamics of variable-viscosity nanofluid flow with heat transfer in a flexible vertical tube under propagating waves. Kishan and Madhu [24] investigated the overall theme of the study the magneto-hydrodynamic mixed convection of a non-Newtonian power-law nanofluid past a moving vertical plate with variable density. Nadeem et al. [25] analyzed the non-Newtonian fluid over stretching surface. The results indicated that the effect of Brownian motion on temperature is increasing. Gupta and Sbragaglia [26] debated the deformation and break-up of viscoelastic droplets using Lattice Boltzmann Models. Ibrahim and Shankar [27] computed MHD boundary layer flow and heat transfer of a nanofluid past a permeable stretching sheet with velocity, thermal and solutal slip boundary conditions. Khan et al. [28] flexed study numerical investigation of magneto-

hydrodynamic stagnation point flow with variable properties. Rana and Bahrgava [29] computed instability of finite element simulation of transport phenomena of viscoelastic nanofluid over a stretching sheet with energy dissipation. Yadav et al. [30] discussed thermal instability in a rotating porous layer saturated by a non-Newtonian nanofluid with thermal conductivity and viscosity variation.

The objective of present study is to illuminate MHD Jeffrey nanofluids flow over a stretching sheet through a porous medium in presence of nonlinear thermal radiation and heat generation/absorption. the self-similar transformations was used to conversion the ruling equations from partial differential equations to ordinary differential equations, which solved numerically by using Runge-Kutta fourth order method, MATLAB was used to get the results of both velocity, temperature, nanoparticles volume fraction and calculate numerical values for skin fraction, local Nusselt number and local Sherwood number.

PROBLEM FORMULATION

Consider two-dimensional steady incompressible flow of MHD non-Newtonian nanofluid on a stretching surface, the flow is assumed to be confined to $y > 0$ while the stretching surface is represented by the plane $y = 0$. On the other hand, the effect of the fluid magnetic field coefficient B_o is in the direction of the y axis with neglected magnetic field induced because Reynolds number of the fluid flow is too small. The temperature of the nanofluid dependent on heat source/sink and thermal radiation. In the present case, the assumption that the surface is stretched with the linear velocity $u_w(x) = ax$ where $a > 0$ is constant and x axis is measured along the stretching sheet. The boundary layer governing equations of Jeffery fluid with nanoparticles are given in the system:

$$\frac{\partial u}{\partial x}+\frac{\partial v}{\partial y}=0 \tag{1}$$

$$u\frac{\partial u}{\partial x}+v\frac{\partial u}{\partial y}=\frac{\nu}{1+\lambda}\left[\frac{\partial^2 u}{\partial y^2}+\lambda_1\left(u\frac{\partial^3 u}{\partial x\partial y^2}-\frac{\partial u}{\partial x}\frac{\partial^2 u}{\partial y^2}+\frac{\partial u}{\partial y}\frac{\partial^2 u}{\partial x\partial y}+v\frac{\partial^3 u}{\partial y^3}\right)\right]-\frac{\sigma}{\rho}B_o^2 u-\frac{\nu}{K}u \tag{2}$$

$$u\frac{\partial T}{\partial x}+v\frac{\partial T}{\partial y}=\alpha\left(\frac{\partial^2 T}{\partial x^2}+\frac{\partial^2 T}{\partial y^2}\right)+\tau\left\{D_B\left(\frac{\partial C}{\partial x}\frac{\partial T}{\partial x}+\frac{\partial C}{\partial y}\frac{\partial T}{\partial y}\right)+\left(\frac{D_T}{T_\infty}\right)\left[\left(\frac{\partial T}{\partial x}\right)^2+\left(\frac{\partial T}{\partial y}\right)^2\right]\right\}-\frac{1}{\rho_{cp}}\frac{\partial q_r}{\partial y}+\frac{Q}{\rho_{cp}}(T-T_\infty) \tag{3}$$

$$u\frac{\partial C}{\partial x}+v\frac{\partial C}{\partial y}=D_B\left(\frac{\partial^2 C}{\partial x^2}+\frac{\partial^2 C}{\partial y^2}\right)+\left(\frac{D_T}{T_\infty}\right)\left(\frac{\partial^2 T}{\partial x^2}+\frac{\partial^2 T}{\partial y^2}\right) \tag{4}$$

Whereas, u is velocity component in x direction and v is velocity component in y direction, ρ_{cp} is the density of base fluid, ρ represents the density of the fluid σ is the electrical conductivity, λ is ratio of relaxation to radiation times, λ_1 is retardation time, ν is the kinematic viscosity of the fluid, α is thermal diffusivity, T is the temperature fluid, C is the nanoparticles volume fraction, D_B is the Brownian diffusion coefficient, D_T is the thermophoresis diffusion coefficient, T_W is the temperature of wall, C_W is the nanoparticles fraction at wall, C is the volumetric volume expansion coefficient, $\tau = (\rho_c)_p/(\rho_c)_f$ is the ratio between the effective heat capacity of the nanoparticles material and heat capacity of the fluid, $q_r = -\frac{4\sigma^*}{3k^*}\frac{\partial T^4}{\partial y}$ is the nonlinear radiativ heat flux via Roseland's approximation when σ^* and k^* are the Stefan-Boltzmann constant and the mean absorption coefficient respectively, when y tends to infinity then the ambient values of T and C are denoted by T_∞ and C_∞. The associate boundary condition for the present problem from 2 to 4 is:

$$u = ax, v = 0, T = T_W,\ D_B\frac{\partial C}{\partial y}+\frac{D_T}{T_\infty}\frac{\partial T}{\partial y}=0 \ when\ \ y=0,\quad u=0,\ v=0,\ T=T_\infty,\ \ C=C_\infty\ \ when\ \ y=\infty. \tag{5}$$

The system of non-linear partial differential equations 1 to 4 converted to system of non-linear ordinary differential equations by the similarity transformation:

$$\psi=\sqrt{a\nu}\ xf(\eta), \theta(\eta)=\frac{T-T_\infty}{T_W-T_\infty}, \varphi(\eta)=\frac{C-C_\infty}{C_W-C_\infty},\quad \eta=\sqrt{\frac{a}{\nu}}\ y \tag{6}$$

Where η is the similarity variable, and ψ, θ and φ are the dimensionless stream function, temperature and concentration respectively. The velocity components $u=\frac{\partial\psi}{\partial y}$ and $v=-\frac{\partial\psi}{\partial x}$. Making use of equation 6, equation of continuity is identically satisfied and the equations from 2 to 4 along with 5 take the flowing form:

$$f'''+\beta\left(f''^2-ff''''\right)+(1+\lambda)\left(ff''-f'^2-Mf'-Da\,f'\right)=0 \tag{7}$$

$$\theta''+Pr\left(Nb\,\theta'\phi'+Nt\,\theta'^2++S\theta+\ f\theta'+R((Ct+\theta)^3\ \theta')'\right)=0 \tag{8}$$

$$\phi''+Le\,(f\,\phi')+\frac{Nt}{Nb}\,\theta''=0 \tag{9}$$

With the boundary condition in form:

$$f(0)=0, f'(0)=1, \theta(0)=1, Nb\phi'(0)+Nt\theta'(0)=0 \tag{10}$$

$$f'(\infty)=0,\ f''(\infty)=0, \theta(\infty)=0\ , \phi(\infty)=0 \tag{11}$$

Where $\beta = \lambda_1 c$ is Deborah number, $Pr = \nu/\alpha$ is Prandtl number. $Nb = \frac{(\rho c)_P D_B (C_W - C_\infty)}{\nu (\rho c)_P}$ is the Brownian motion, $Nt = \frac{(\rho c)_P D_T (T_W - T_\infty)}{\nu (\rho c)_P}$ is the thermophoresis, $Le = \nu/D_B$ is the Lewis number, $M = \frac{\sigma B_0^2}{a\rho}$ is the magnetic field, $Da = \frac{\nu}{aK}$ is the Darcy number, $S = \frac{Q}{a\rho_f c_p}$ is the heat source, $Ct = \frac{T_\infty}{T_W - T_\infty}$ is the ratio between the temperature of the wall and the difference between infinity temperature and the temperature of the wall. C_f , Nu and Sh Represents skin fraction, Local Nusselt number and local Sherwood number respectively, are defined as:

$$Nu = \frac{x q_W}{\alpha (T_W - T_\infty)} \ , \quad Sh = \frac{x q_m}{D_B (C_W - C_\infty)} \ = 0 \ , \\ C_f = \left(1 + \frac{1}{\beta}\right) \frac{\mu}{\rho u_w^2} \left[\frac{\partial u}{\partial y}\right]_{y=0} \tag{12}$$

Where q_W and q_m are the heat flux and mass flux respectively.

$$\frac{q_W}{-\alpha} = \left(\frac{\partial T}{\partial y}\right)_{y=0} \ , \ \frac{q_m}{-D_B} = \left(\frac{\partial C}{\partial y}\right)_{y=0} \tag{13}$$

Dimensionless form of equation 12 can be written on the formula:

$$-\theta'(0) = \frac{Nu}{Re_x^{\frac{1}{2}}} \ , -\phi'(0) = \ \frac{Sh}{Re_x^{\frac{1}{2}}} \ , C_f = \frac{\left(1+\beta^{-1}\right) f''(0)}{Re_x^{1/2}} \tag{14}$$

Where $Re_x = \frac{1}{\nu}(x U_W(x))$ is local Reynolds number based on the stretching velocity $U_W(x)$.

NUMERICAL SOLUTION

The system of non-linear coupled differential equations (7-9) with boundary conditions (10-12) are solved numerically by using Runge-Kutta fourth-order method with a shooting technique.

$\Delta\eta = 0.001$ Is the step which used to obtain the numerical solution with η_{max}. The system of normal differential equations governing was introduced within the MATLAB program in a certain way:

$$f = Y(1)$$

$$f' = F(1) = Y(2)$$

$$f'' = F(2) = Y(3)$$

$$f''' = F(3) = Y(4)$$

$$f'''' = F(4) = \Big(Y(4) + \beta \times Y(3)^2 + (1+\lambda) \times \big(Y(1) \times Y(3) - Y(2)^2 - M \times Y(2) - Da \times Y(2)\big)\Big) / (\beta \times Y(1));$$

$$\theta = Y(5)$$

$$\theta' = F(5) = Y(6)$$

$$\theta'' = F(6) = \Big(-Pr \times \Big(Nb \times Y(6) \times Y(8) + Nt \times Y(6)^2 + S \times Y(5) + Y(1) \times Y(6) + 3 \times R \times \big(Ct + Y(5)\big)^2 \times Y(6)^2\Big)\Big) / \big(1 + Pr \times R \times \big(Ct + Y(5)\big)^3\big) ;$$

$$\phi = Y(7)$$

$$\phi' = F(7) = Y(8)$$

$$\phi'' = F(8) = -Le * Pr * Y(1) * Y(8) - \left(\frac{Nt}{Nb}\right) * F(6)$$

The effect of all important physical factors on the velocity, temperature and concentration of nanoparticles was studied and treated. On the other hand, these important effects were studied by making graphs of each physical factor through which a thorough and accurate study can be done. In order to verify the accuracy of the numerical results of the current work, we made a numerical comparison in Tables 1 and 2 between the results of the current work corresponding to the local Sherwood and Nusselt numbers in case of $Pr = 10, Le = 1$ and absence of all the parameters with the published results available for Nadeem et al. [25] in order to give confidence and accuracy in the numerical results obtained.

Table 1
Comparisons between the numerical values of the local Nusselt number for Nadeem et al. [25] and our present study in the absence each of β , λ , Da , S , M , Ct and R when $Le = 1$ and Pr $= 10$.

	Nt = 0.1		**Nt = 0.3**		**Nt = 0.5**	
	Nadeem et al. [25]	**Present study**	**Nadeem et al. [25]**	**Present study**	**Nadeem et al. [25]**	**Present study**
Nb	$-\theta'(0)$	$-\theta'(0)$	$-\theta'(0)$	$-\theta'(0)$	$-\theta'(0)$	$-\theta'(0)$
0.1	1.7100	1.7222	1.3029	1.2993	0.9901	0.9795
0.3	1.1442	1.1433	0.8458	0.8424	0.6280	0.6118
0.5	0.7088	0.7028	0.5093	0.5034	0.3707	0.3643
0.7	0.4021	0.3952	0.2821	0.2801	0.2021	0.1959

It is worth mentioning that a numerical study of the impact of important parameters and calculation of numerical values was done for each of Local Nusselt number, Local Sherwood number and skin fraction and this is represented in Table 3 it

is concluded that Coefficient of skin friction is increasing by increasing the values of magnetic field *M*, Darcy number *Da* and ratio of relaxation to retardation times λ while there is a decrease in the coefficient of skin friction when the increase in values Deborah number β.

Table 2

Comparisons between the numerical values of the local Sherwood number for Nadeem et al. [25] and our present study in the absence each of $\beta, \lambda, Da, S, M, Ct \text{ and } R$ when $Le = 1 \text{ and } \Pr = 10$.

	Nt = 0.1		**Nt = 0.3**		**Nt = 0.5**	
	Nadeem et al. [25]	**Present study**	**Nadeem et al. [25]**	**Present study**	**Nadeem et al. [25]**	**Present study**
Nb	$-\phi'(0)$	$-\phi'(0)$	$-\phi'(0)$	$-\phi'(0)$	$-\phi'(0)$	$-\phi'(0)$
0.1	-0.7636	-0.7458	-2.3086	-2.2398	-2.7982	-2.6633
0.3	0.3114	0.3330	0.0422	0.0741	0.0031	0.0669
0.5	0.4998	0.5202	0.4395	0.4657	0.4585	0.4910
0.7	0.5620	0.5813	0.5630	0.5873	0.5914	0.6198

As for the values of the local Nusselt number, it was found that it decreases with all the values of the parameters, as opposed to the Prandtl and Lewis numbers. Finally, when looking at the values of the local Sherwood number, it was found that it increases with all values of all parameters in contrast to the Prandtl and Lewis numbers.

Table 3

The numerical values of the local Nusselt number, local Sherwood number and Skin fraction for each of $\beta, \lambda, Da, S, M, Ct, R, Le, Pr, Nb \text{ and } Nt$.

β	**M**	**Da**	**λ**	**R**	**Nb**	**Nt**	**S**	**Ct**	**Pr**	**Le**	$-\theta'(0)$	$-\phi'(0)$	$-f''(0)$
1	0.6	0.5	0.5	0.5	0.5	0.5	-0.1	1.2	5	2	0.17935	-0.17935	0.96919
1.5											0.18609	-0.18609	0.88419
2											0.19058	-0.19058	0.82596
1	1										0.17585	-0.17585	1.02554
	1.5										0.17233	-0.17233	1.08692
	2										0.16949	-0.16949	1.14083
	0.6	1									0.17508	-0.17508	1.03853
		1.5									0.17172	-0.17172	1.09823
		2									0.16898	-0.16898	1.15088
		0.5	1								0.17351	-0.17351	1.06508
			1.5								0.16928	-0.16928	1.14366
			2								0.16603	-0.16603	1.21073
			0.5	0.1							0.45611	-0.45611	0.96919
				0.2							0.31216	-0.31216	0.96919
				0.3							0.24587	-0.24587	0.96919
				0.5	0.1						0.18076	-0.90380	0.96919
					0.3						0.17935	-0.29892	0.96919
					0.7						0.17935	-0.12810	0.96919
					0.5	0.9					0.17367	-0.31261	0.96919
						1.3					0.17019	-0.44251	0.96878
						1.7					0.16557	-0.56296	0.96878
						0.5	-0.3				0.24119	-0.24119	0.96919
							-0.2				0.21289	-0.21289	0.96919
							0				0.13594	-0.13594	0.96919
							-0.1	0.5			0.33263	-0.33263	0.96919
								0.7			0.27515	-0.27515	0.96919
								1			0.21117	-0.21117	0.96919
								1.2	9		0.18060	-0.18060	0.96919
									13		0.18109	-0.18109	0.96919
									17		0.18135	-0.18135	0.96919
									5	3	0.17881	-0.17881	0.96919
										4	0.17997	-0.17997	0.96878
										5	0.17980	-0.17980	0.96878

RESULTS AND DISCUSSIONS

In the present study it will be investigate the influences of eleven physical parameters that are as follows, the Deborah number β, the ratio of relaxation to retardation times parameter λ, the Brownian motion parameter Nb, the thermophoresis parameter Nt , the Prandtl number parameter Pr, the Lewis number parameter Le, the magnetic field parameter M, the Darcy number parameter Da, the non-linear thermal Radiation parameter R, the heat source/sink parameter S, the ratio between the temperature of the wall and the difference between infinity temperature and the temperature of the wall Ct, on each of velocity $f'(\eta)$, temperature $\theta(\eta)$ and nanoparticles volume fraction $\phi(\eta)$.

Velocity profiles

The degree of viscosity of non-Newtonian fluids and the property of resistance within them are closely related to the Deborah number β.

The higher the values of this number, the greater the degree of viscosity and resistance of this fluid. In examining the effect of this number on the velocity distribution of the Jeffrey fluid, a significant enhancement of the velocity distribution was observed with a significant reduction in the boundary layer, all this can be seen in Figure 1.

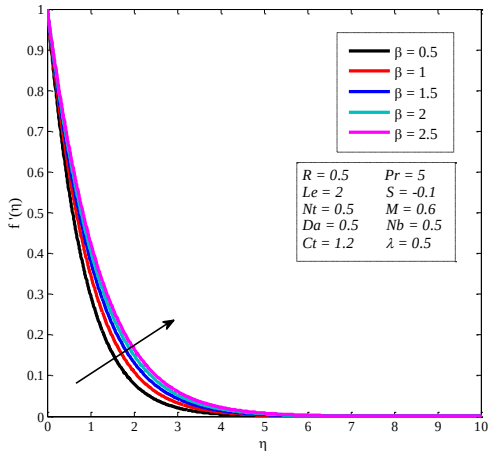


Fig. 1. Effect of the Deborah number β on the velocity profile

As for study of influence of the magnetic field parameter M, this is represented by the Figure 2 which illustrates the effect of this important physical coefficient on the distribution of velocity it is noted the increase in the magnetic field means the decrease and slows in the fluid velocity and this explains that the relationship between them is inverse.

Physically the study of flow and heat transfer of an electrically conductive liquid in the presence of a magnetic field in the sense that dynamic magnetic flow through a hot surface has applications in manufacturing processes such as plate cooling, nuclear reactor, extrusion of polymers, in many metal processes such as drawing continuous filaments through quiet liquids, and solidification.

The copper wire is darkened, the product finish characteristics largely depends on the cooling rate involved in these processes.

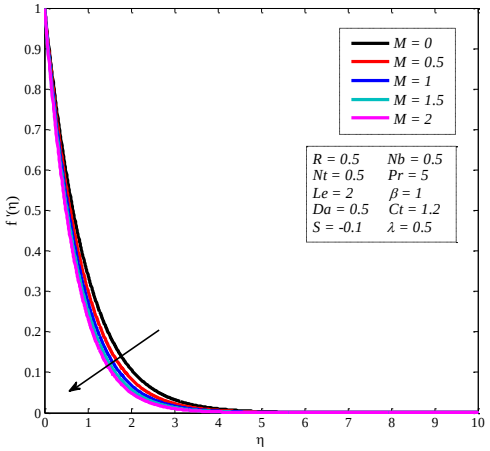


Fig. 2. Effect of the magnetic field M on the velocity profile

Figure 3 represents the change in the fluid velocity in the case of different values taken by the Darcy number Da, it is noticed that the increase in the Darcy number negatively affect the fluid velocity.

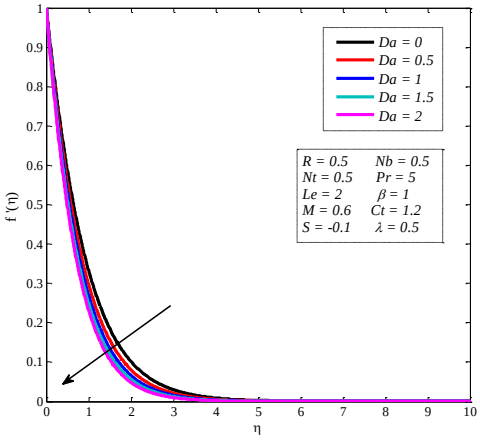


Fig. 3. Effect of the Darcy number Da on the velocity profile

Physically it is known that the Darcy number is associated with porosity of porous media and the higher the porosity of the porous medium, the lower the permeability of the fluid, which makes the velocity slow.

On the other hand, Figure 4 analyzed the effect of the ratio of relaxation to radiation times λ on velocity is decreasing when promoting values of λ.

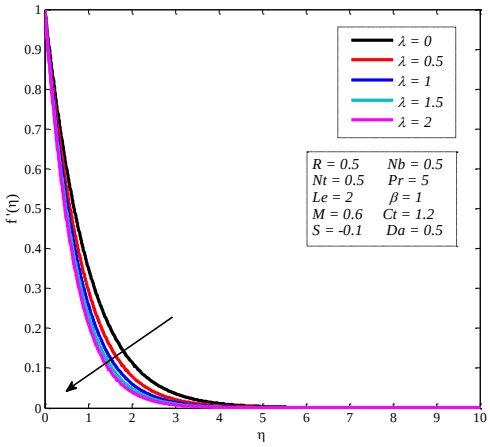


Fig. 4. Effect of λ parameter on the velocity profile

Temperature distributions

Figure 5 investigates the impact of Deborah number β on the temperature distribution, it can be seen that the higher value of β corresponds to the decrease in the fluid temperature.

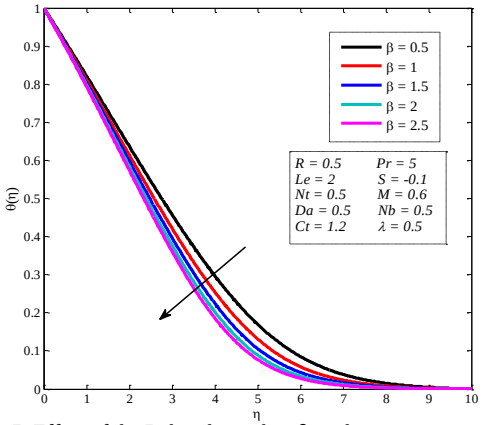


Fig. 5. Effect of the Deborah number β on the temperature profile

Figures 6 and 7 show the variation in temperature distribution for different values each of the magnetic field and M and the Darcy number Da parameters respectively.

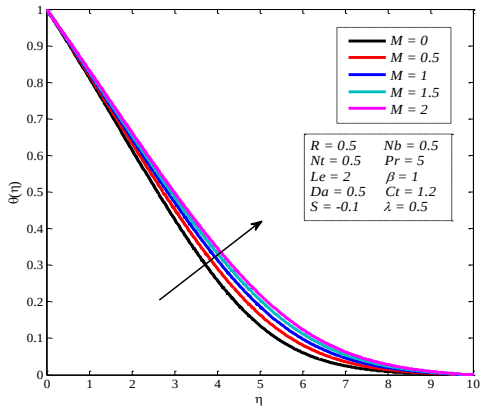


Fig. 6. Effect of the magnetic field M on the temperature profile

here M represent hydromagnetic flow because $M > 0$, it is noticed the temperature profiles is strong when the magnetic field and Darcy number take a higher values, in addition to it makes the thermal boundary layer thickness is strong, that is show the relationship between each of the magnetic field and Darcy number with the temperature are a positive relationship.

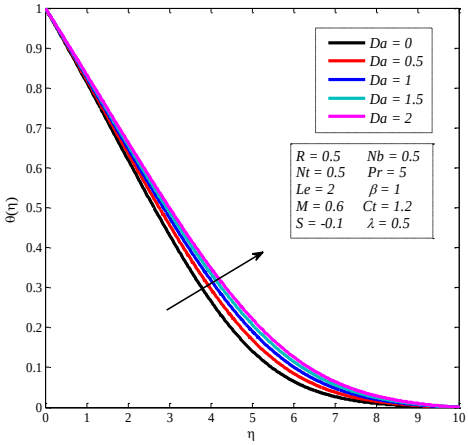


Fig. 7. temperature profile for variations of the Darcy number parameter Da

Physically, the magnetic field parameter depends on the Lorentz force that caused to a growing in the temperature and thermal boundary layer thickness.

Figures 8 and 9 presents the impacts of both the non-linear thermal radiation parameter R and the ratio temperature Ct on the temperature distribution, it is observed a significant Strengthen in fluid temperature for the large values of both R and Ct.

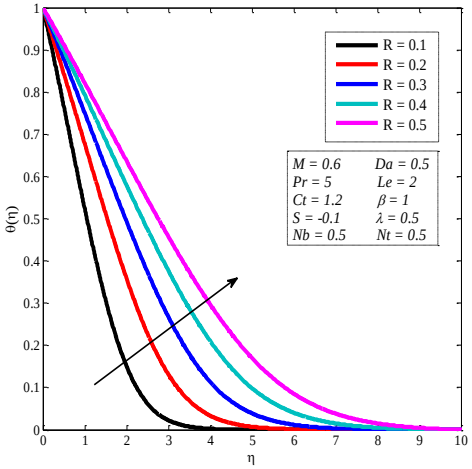


Fig. 8. temperature profile for variations of the thermal radiation parameter R

Physically, it is clear that the relationship between thermal radiation and temperature ratio is a direct relationship that plays an important role in the temperature

difference so that the large values taken by thermal radiation and temperature ratio led to raise the surface temperature, which made the temperature of the fluid is high and on the other side, the large values of non-linear thermal radiation parameter shows a growing in the thermal boundary layer thickness, the thermal radiation effect plays a significant role in controlling heat transfer process in polymer processing industry.

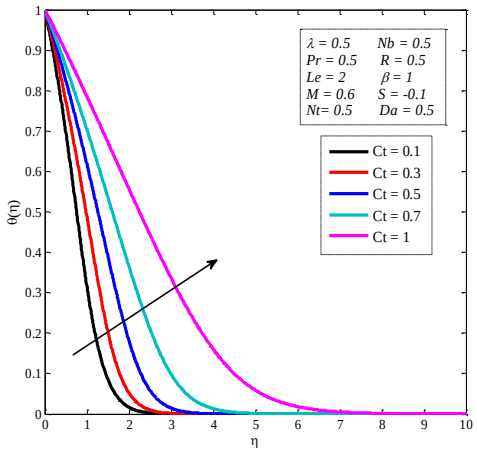


Fig. 9. temperature profile for variations of the parameter *Ct*

The quality of the final product depends to a certain extent on heat controlling factors. Also, the effect of thermal radiation on flow and heat transfer processes is of major important in the design of many advanced energy convection systems which operate at high temperature. Prandtl number is one of the important parameter in the fluid dynamics and from a physical point of view it can be defined as the ratio of the viscous diffusion rate to the thermal diffusion rate expressed as the ratio of kinematic viscosity to the thermal diffusivity the effect of the Prandtl number *Pr* on the temperature profiles is displayed in Figure 10 it is clear that as the Prandtl number *Pr* increases, the temperature decreases.

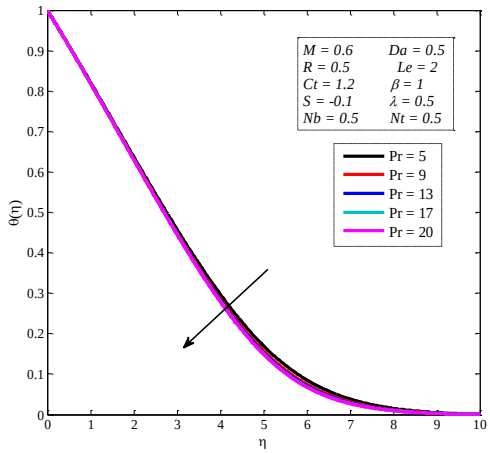


Fig. 10. temperature profile for variations of the Prandtl number parameter *Pr*

Physically *Pr* is dependent only on the fluid and not on the surface on which the fluid flow the increase of Prandtl number leads to a decreasing thermal boundary layer thickness and more regular temperature distribution across the boundary layer.

When reviewing Figure 11, note the effect of the parameter of the most important parameters through which the enhancement occurs in the temperature of the fluid which is an effect of thermophoresis Nt this resulted in a significant boost in fluid temperature rise when taking large values.

Physically the thermophoresis force is the force that moves the fluid molecules from the center of high temperature to the center of low temperature and this is called positive force, on the other hand, this force increases the density and thickness of the thermal boundary layer, which also leads to the acquisition of nanoparticles thermal energy increases the movement.

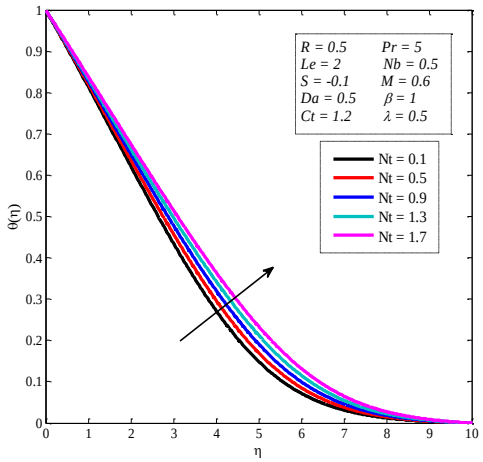


Fig. 11. temperature profile for variations of the thermophoresis parameter *Nt*

The impact of the heat source/sink parameter *S* can be found in Figure 12, for $S > 0$ (type of heat source) it can be observed that the boundary layer generates heat energy, which is enough reason to make the temperature of the border layer high and the temperature of the fluid is also high, whereas $S < 0$ (type of heat sink).

In this case it is conclude a decrease in the temperature of the fluid and also a decrease in the temperature of the boundary layer, which is called the state of absorption of thermal energy.

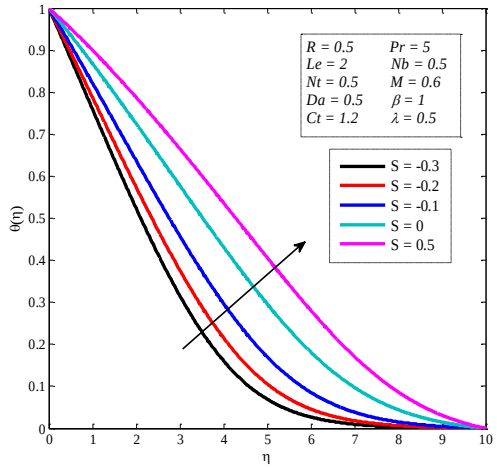


Fig. 12. temperature profile for variations of the heat source/sink parameter S

Finally as for the temperature distribution it increases when the values increase in the ratio relaxation time λ this is illustrated by Figure 13.

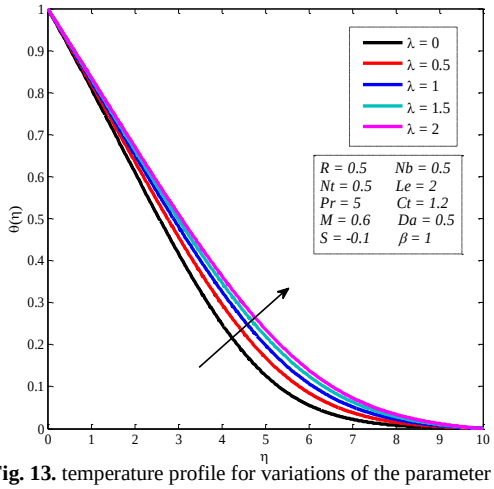


Fig. 13. temperature profile for variations of the parameter λ

Nanoparticles distributions

The effect of the Prandtl number Pr on the distribution of nanoparticle concentration is shown in Figure 14 which shows that the increase in the Prandtl number leads to a reduction in the concentration of nanoparticle fluid molecules so close to the boundary layers and the rubber surface.

In case of know the extent of the change in the nanoparticles concentration of fluid through the influence of the Lewis number Le.

Firstly, the Lewis number is defined as the ratio of thermal diffusivity and mass diffusivity and it is used to study fluid flow discrimination in the case of heat and mass transfer and to determine the ratio between them.

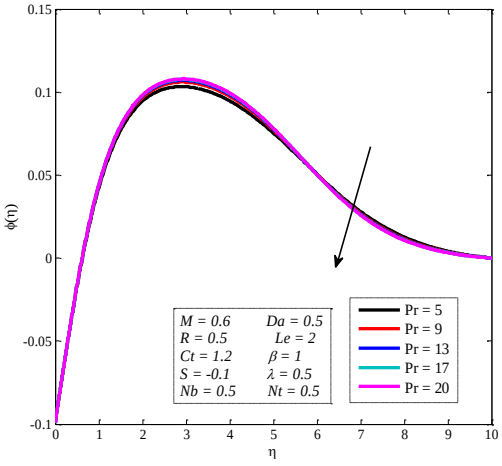


Fig. 14. effect of the Prandtl number parameter Pr on the concentration distribution

On the other hand, it plays an important role in determining the thickness of the thermal boundary layer, so Figure 15 shows that the increase in Lewis number leads to a decrease in the distribution of nanoparticles concentration. Physically an increase in the Lewis number means a decrease in concentration and this leads to a decrease in mass flow rate. On the other hand, low values of Le lead to a decrease in the thickness of the boundary layer and an increase in the mass flow rate.

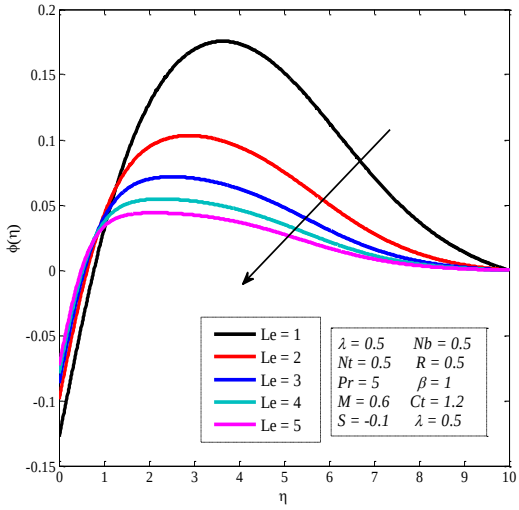


Fig. 15. effect of the Lewis number parameter Le on the concentration distribution

Figure 16 explain the effect of the thermophoresis parameter Nt on the concentration of nanoparticles distribution, since the positive effect of the thermophoresis parameter is offset by a positive effect on the concentration of nanoparticle distribution. Physically an increase in the values of the thermophoresis parameter means an increase in the thermal energy gained by nanoparticles, which in turn

enhance the transport of these molecules in such a way that their concentration is large.

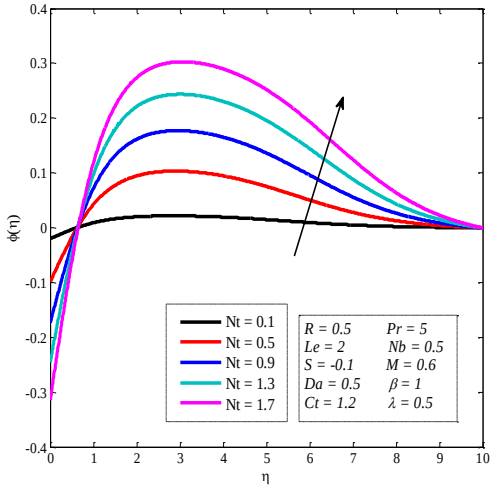


Fig.16. effect of thermophoresis parameter Nt on the concentration distribution

Figures 17 and 18 elucidate impacts of the heat generation/absorption S and the ratio radiation parameter Ct on the concentration of nanoparticles distribution.

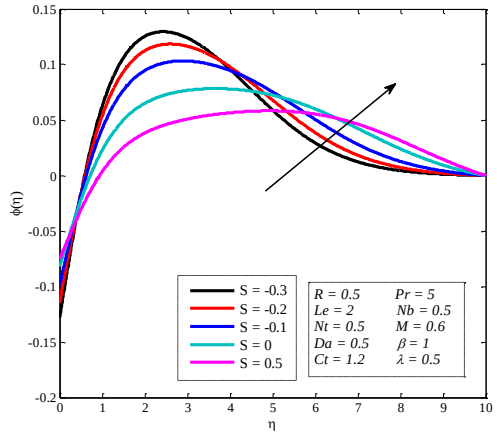


Fig.17. effect of the heat source/sink parameter S on the concentration distribution

Firstly in Figure 17 it is found that in the case of heat absorption, the temperature of the boundary layer decreases, leading to the low temperature of nanoparticles as well decreasing its velocity and decreasing its concentration, the opposite happens in the case of heat generation. Secondly in Figure 18 the effect of Ct parameter on the concentration of nanoparticles distribution is positive it is meaning that growth the concentration of nanoparticles distribution.

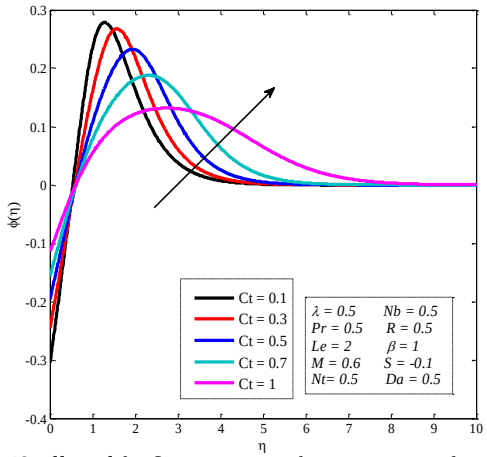


Fig.18. effect of the Ct parameter on the concentration distribution

According to the influence of the Brownian motion Nb in the nanoparticles volume fraction in Figure 19 it reduces the concentration and movement of nanoparticles in the fluid.

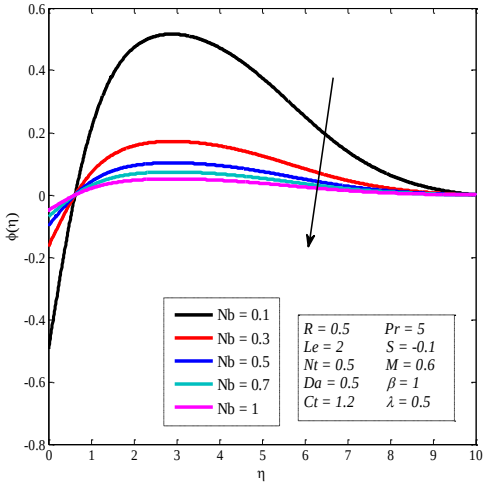


Fig.19. effect of Brownian motion parameter Nb on the concentration distribution

Physically in nanofluid system, the pattern of movement of nanoparticles within the fluid follows a random pattern in the sense that these molecules move in all directions randomly so that the increased concentration of nanoparticles was the result of increased values of thermophoresis and this is offset by a decrease in Brownian motion coefficient and increase in the thickness of the boundary layer. Finally in Figures 20, 21 and 22 respectively are shows important study of variations in the nanoparticles volume fraction when the magnetic field, the Darcy number and ratio relaxation time takes large values.

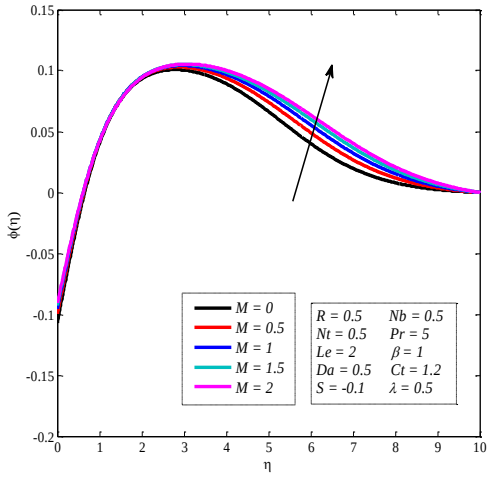


Fig.20. effect of magnetic field parameter *M* on the concentration distribution

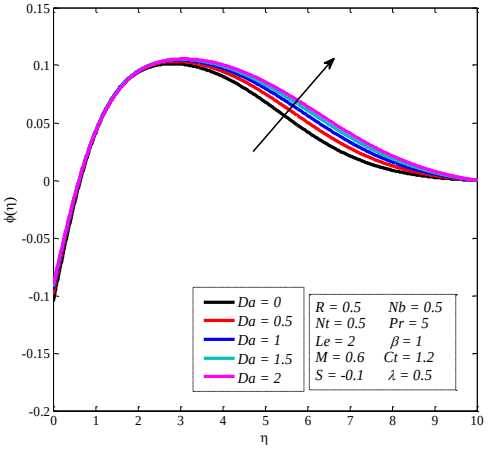


Fig.21. effect of Da parameter on the concentration distribution

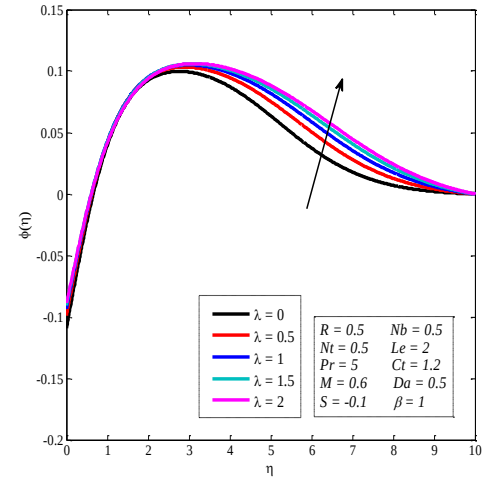


Fig.22. effect of λ parameter on the concentration distribution

It was found that the effects of these parameters when they take large values consistent in their effect on the distribution of nanoparticles in that they increase the concentration of these molecules within the fluid.

Profiles of skin friction, local Nusselt and Sherwood numbers

Figure 23 analyses the impacts each of Darcy number *Da* and magnetic field *M* on the skin friction profiles, an increase in the values each of Darcy number and magnetic field leads to the skin friction coefficient became large.

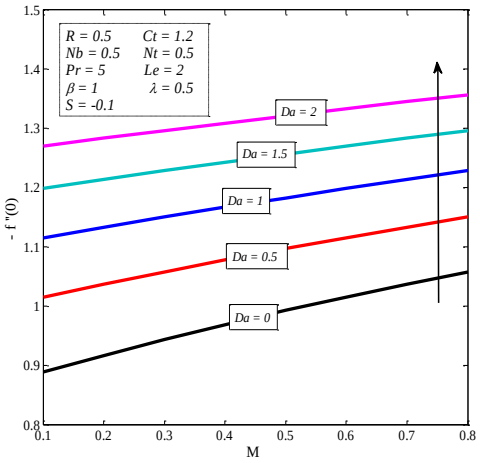


Fig.23. effect of Darcy number and magnetic field on the skin fraction $-f''(0)$

On the other hand when viewing the Figures 24 and 25 it is note that the effect on local Nusselt number becomes negative when increasing the values of both the heat source/sink S, non-linear thermal radiation R and Ct parameter, but in Figures 26 and 27 the impact on local Sherwood number become positive.

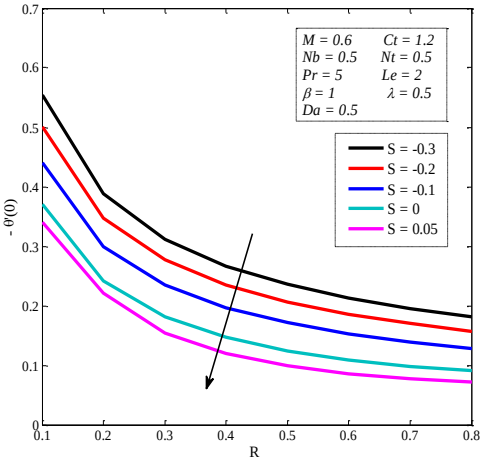


Fig.24. effect of heat source/sink *S* and radiation parameters *R* on the Local Nusselt number $-\theta'(0)$

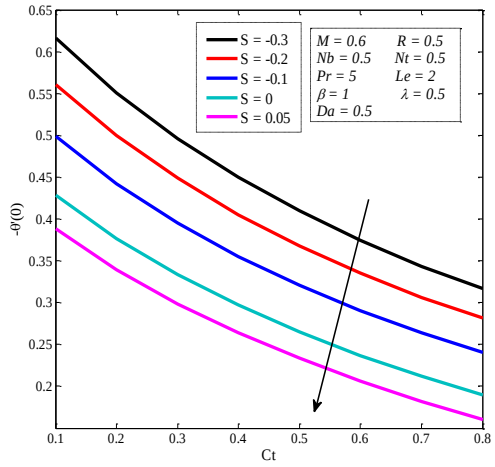


Fig. 25.effect of heat source/sink *S* and *Ct* parameters on the Local Nusselt number $-\theta'(0)$

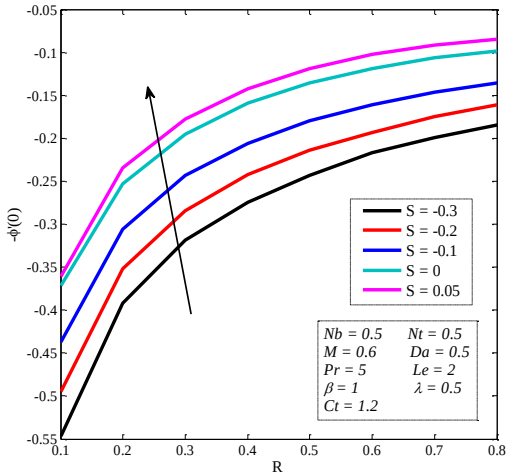


Fig. 26. effect of heat source/sink *S* and *R* parameters on the Local Sherwood number $-\phi'(0)$

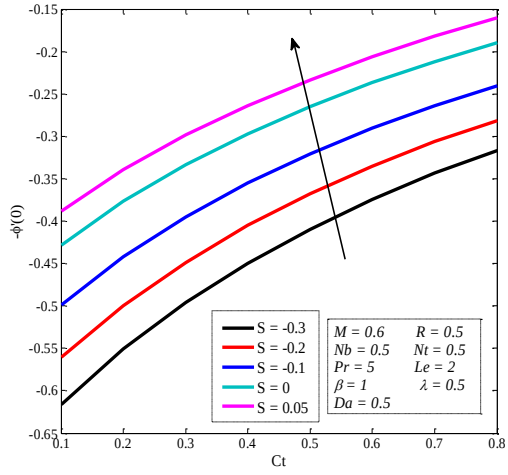


Fig. 27. effect of heat source/sink *S* and *Ct* parameters on the Local Sherwood number $-\phi'(0)$

CONCLUSIONS

In present study we reviewed the MHD Jeffrey nanofluids flow over a stretching sheet through a porous medium in presence of nonlinear thermal radiation and heat generation/absorption. Numerical solutions for velocity, temperature and nanoparticles distributions were progressed and discussed. All that we have deduced from this study can be mentioned in the following points:

1. The effects each of magnetic field M, Darcy number Da and ratio relaxation λ time on velocity distribution was negatively while the impact of Deborah number β was positively.
2. The influences each of magnetic field M, Darcy number Da and ratio relaxation λ time on the temperature distribution was positively while the impact of Deborah number β was negatively.
3. The temperature distribution was increased by increasing in each of nonlinear thermal radiation coefficient R, thermophoresis Nt, heat source/sink S and Ct parameter values while the effect of the Prandtl number on the temperature distribution was decreasing.
4. The concentration distribution of nanoparticles was increasing in case of increase in values each of thermophoresis Nt, heat source/sink S, Darcy number Da, Magnetic field M and λ, Ct parameters, on the other hand effects of both Prandtl number Pr, Lewis number Le and Brownian motion Nb made the concentration of nanoparticles weak.
5. The increase in the effect of both the magnetic field M and the Darcy number Da worked on growth the skin fraction, on the other side increase in the effects of both thermal radiation R, heat source/sink S and Ct parameter was decreasing on the Local Sherwood number and increasing on Local Nusselt number.

Acknowledgment

The authors would like to extend their appreciation to the Deanship of Scientific Research at King Khalid University for administration and technical support.

REFERENCE

[1] Gangaiah T, Saidulu N, Lakshmi AV. Magnetohydrodynamic flow of nanofluid over an exponentially stretching sheet in presence of viscous dissipation and chemical reaction. J. Nanofluids 2018; 7: 439–448.

[2] Farooq M, Javed M, jaz Khan M I, Anjum A, Hayat T. Melting heat transfer and double stratification in stagnation flow of viscous nanofluid. J. Results in Physics, 2017; 7: 2296-2301.

[3] Hsiao KL, MHD Stagnation electrical MHD nanofluid mixed convection with slip boundary on a

stretching sheet. J.Applied Thermal Engineering, 2016; 98: 850-861.

[4] Mabood F, Ibrahim SM, Khan WA. Framing the features of Brownian motion and thermophoresis on radiative nanofluid flow past a rotating stretching sheet with magnetohydrodynamic. J. Results in Physics. 2016; 6: 1015-1023.

[5] Ansari MS, Motsa SS, Trivedi M. A new numerical Approach to MHD Maxwellian nanofluid flow Past an impulsively stretching sheet. J. Nanofluids. 2018; 7: 449–459.

[6] Nampelly S, Lakshmi AV, Tulishetti G. Thermal radiation and slip effects on MHD flow and heat transfer of Casson nanofluid over an exponentially stretching sheet. J.Nanofluids. 2018; 7: 478–487.

[7] Goyal M, Bhargava R. Boundary layer flow and heat transfer of viscoelastic nanofluids past a stretching sheet with partial slip conditions. J. Applied Nanoscience.2014; 4: 761–767.

[8] Krishnamurthy MR , Prasannakumara BC, Gireesha BJ, Gorla RSR. The effect of chemical reaction on MHD boundary layer flow and melting heat transfer of Williamson nanofluid in porous medium. Int. J. Engineering Science and Technology.2016; 19: 53-61.

[9] Bhargava R, Rana P. Finite element analysis of viscoelastic nanofluid flow with energy dissipation and internal heat Source/Sink effects. J. Information and Operations Management. 2017; 3: 1421–1447.

[10] Madhua M, Kishanb N. Finite Element Analysis of MHD viscoelastic nanofluid flow over a stretching sheet with radiation. Int. J. Heat and Mass Transfer. 2015; 127: 432 – 439.

[11] Chanie AG, Shankar B, Nandeppanavar MM. MHD flow of nanofluids through a porous media due to a permeable stretching sheet . J. Nanofluids.2018; 7, 488–498.

[12] Gaikwad SN, Chillal S. Radiation effect on MHD mixed convective flow of Cu/CuO-Water nanofluids in the presence of chemical reaction . J. Nanofluids.2018; 7: 509–515.

[13] Thumma T, Mishra SR. Effect of viscous dissipation and Joule heating on magnetohydrodynamic Jeffery nanofluid flow with and without multi slip boundary conditions. J. Nanofluids.2018; 7: 516–526.

[14] Zeid MA, Effects of thermal-diffusion and viscous dissipation on peristaltic flow of micropolar non-Newtonian nanofluid. J. Results in Physics. 2016; 6: 481-495.

[15] Mliki B, Abbassi MA, Guedri K, Omri A. Lattice Boltzmann simulation of natural convection in an L-shaped enclosure in the presence of nanofluid. Int. J. Engineering Science and Technology. 2015; 18: 503-511.

[16] Mohamed RA, Rida SZ, Arafa AAM, Mubark MS. MHD flow of sisko fluid over a bidirectional radiating stretching surface embedded in a nanofluid saturated porous media in the presence of heat generation/absorption and chemical Reaction. J. Nanofluids.2018; 7: 556–569.

[17] Baag S, Mishra SR, Hoque MM, Anika NN. Magnetohydrodynamic boundary layer flow over an exponentially stretching sheet past a porous medium with uniform heat source. J. Nanofluids.2018; 7: 570–576.

[18] Eldabe NTM, Shaker MO, Maha SA. Peristaltic flow of MHD Jeffrey fluid through porous medium in a vertical channel with heat and mass transfer with radiation. J. Nanofluids.2018; 7: 595–602.

[19] Kiran P. Nonlinear thermal convection in a viscoelastic nanofluid saturated porous medium under gravity modulation. J. Ain Shams Engineering. 2016; 7: 639-651.

[20] Naramgari S, Sulochana C, MHD flow of dusty nanofluid over a stretching surface with volume fraction of dust particles. J. Ain Shams Engineering. 2016; 7: 709–716.

[21] Uddin MJ, Rana P, Bég OA, Ismail AIM. finite element simulation of magneto hydrodynamic convective nanofluid slip flow in a porous medium with nonlinear thermal radiation. J. Alexandria Engineering . 2016; 55:1305-1319.

[22] Ganesh NV, Ganga B, Hakeem AKA. Lie symmetry group analysis of magnetic field effects on free convective flow of a nanofluid over a semi-infinite stretching sheet. J. Egyptian Mathematical Society, 2014; 22: 304-310.

[23] Huda AB, Akbar NS, Beg OA, Khan MY. Dynamics of variable-viscosity nanofluid flow with heat transfer in a flexible vertical tube under propagating waves. J. Results in Physics, 2017; 7: 413-425.

[24] Kishan N, Madhu M. magneto-hydrodynamic mixed convection of a non-Newtonian power-law nanofluid past a moving vertical plate with variable density. J. Nigerian Mathematical Society. 2016; 35: 199-207.

[25] Nadeem M, Haq RU, Khan ZH. Non-Newtonian fluid over stretching surface. J. Appl. Nanosci. 2014; 4: 625 – 631.

[26] Gupta A, Sbragaglia M. Deformation and break-up of Viscoelastic Droplets Using Lattice Boltzmann Models. J. Procedia IUTAM. 2015; 15: 215-227.

[27] Ibrahim W, Shankar B. boundary layer flow and heat transfer of a nanofluid past a permeable stretching sheet with velocity thermal and solutal slip boundary conditions. J. Computers & Fluids. 2013; 75: 1–10.

[28] Khan MI, Kiyani MZ, Malik MY, Yasmeen MY, Khan MWA, Abbas T. Study numerical investigation of magnetohydrodynamic stagnation

point flow with variable properties. J. Alexandria Engineering. 2016; 55: 2367-2373.

[29] Rana P, Bahrgava R, Finite element simulation of transport phenomena of viscoelastic nanofluid over a stretching sheet with energy dissipation. J. Information and Operations Management. 2012; 25: 158-161.

[30] Yadav D, Bhargava R, Agrawal GS, Yadav N, Lee J, Kim MC. Thermal instability in a rotating porous layer saturated by a non-Newtonian nanofluid with thermal conductivity and viscosity variation. J. Microfluid Nanofluid. 2014; 16: 425–440.